

Sequential Phase Linking: Progressive Integration of SAR Images for Operational Phase Estimation

Dana El Hajjar, Guillaume Ginolhac, Mohammed Nabil El Korso, Yajing Yan

SLSIP Workshop, Porquerolles

May 15, 2024

1 SAR interferometry

2 Phase Linking (PL)

3 Sequential problematic

4 Covariance fitting interferometric PL (COFI-PL)

- Offline approach
- Online approach

5 PL based on maximum likelihood estimation (MLE-PL)

- Offline approach
- Online approach

6 Conclusion and perspectives

SAR image

Single Look Complex (SLC) is characterized by a complex signal $z = a \cdot e^{j\theta}$

- **Amplitude (a)** : Intensity of the backscattering
- **Phase (θ)**: geometric information, random information
 $\theta = \theta_{\text{random}} + \theta_{\text{geometric}}$

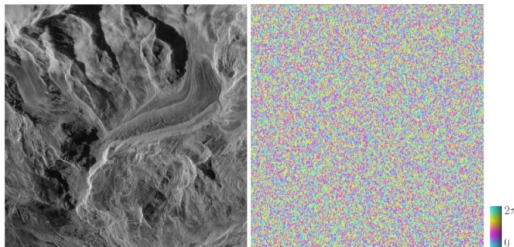


Figure: Sentinel-1 SAR image - glacier

Interferogram

2 SLC images of the **same scene at different times** → interferogram:

$$\gamma e^{j\theta}(i,j) = \frac{\sum_{i,j \in \Omega} z_1(i,j)z_2^*(i,j)}{\sqrt{\sum_{i,j \in \Omega} z_1(i,j)z_1^*(i,j) \sum_{i,j \in \Omega} z_2(i,j)z_2^*(i,j)}}$$

where:

- γ is **coherence** ($\in [0, 1]$), representing the similarity between the two images. It is a measure of the quality of the interferogram
- θ represents the **phase difference** ($\theta = \theta_1 - \theta_2, \theta \in [-\pi, \pi]$)
- Ω represents the spatial neighborhood around pixel (i,j)

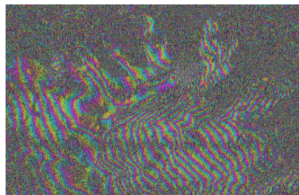
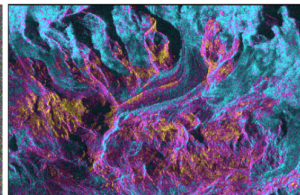


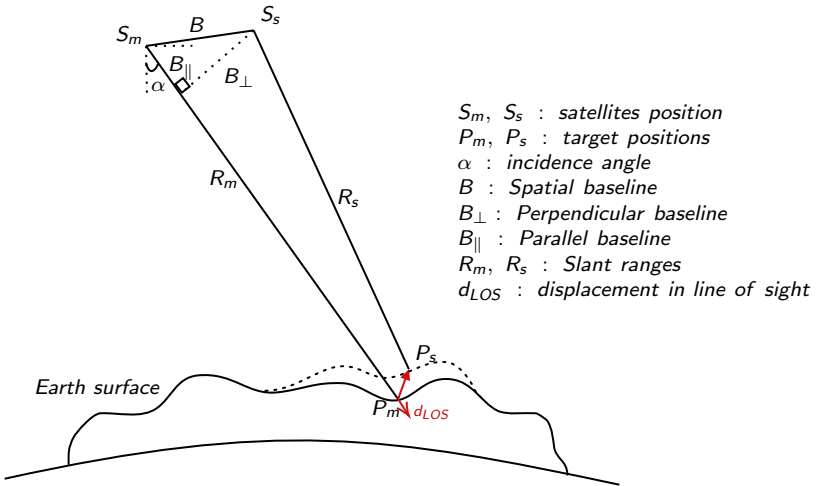
Figure: (a) phase

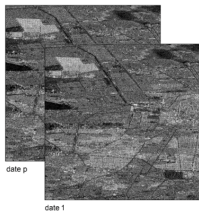


(b) coherence

Interferometric phase

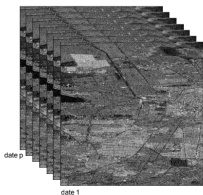
$$\theta = \frac{4\pi}{\lambda} \frac{B_{\perp}}{R_m \sin(\alpha)} h + \frac{4\pi}{\lambda} d_{LOS}$$





Interferogram of 2 SLC images

- Unsatisfactory results
- Measurement accuracy (centimetric)



Multi-temporal interferograms

- Continuous monitoring of Earth deformations
- Improvement in measurement accuracy (millimetric)
- Building interferometric networks from a time series of SAR images

Content

1 SAR interferometry

2 Phase Linking (PL)

3 Sequential problematic

4 Covariance fitting interferometric PL (COFI-PL)

- Offline approach
- Online approach

5 PL based on maximum likelihood estimation (MLE-PL)

- Offline approach
- Online approach

6 Conclusion and perspectives

Data model

Consider a multivariate random vector $\tilde{\mathbf{x}} = [\tilde{x}_1, \dots, \tilde{x}_p]^T$ for all $(l, k) \in [0, p - 1]^2$.

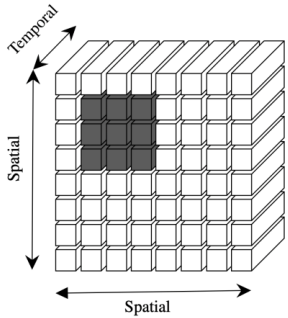
$$\mathbb{E}[\tilde{x}_l(\tilde{x}_k)^*] = \gamma_{k,l}\sigma_k\sigma_l \exp(j(\theta_l - \theta_k))$$

$$\mathbb{E}[\tilde{\mathbf{x}}\tilde{\mathbf{x}}^H] \triangleq \tilde{\boldsymbol{\Sigma}} = \tilde{\boldsymbol{\Psi}} \odot \tilde{\mathbf{w}}_\theta \tilde{\mathbf{w}}_\theta^H \quad (1)$$

with:

- $\gamma_{k,l}$: correlation coefficient between \tilde{x}_k and \tilde{x}_l
- σ_l : standard deviation of \tilde{x}_l
- $\tilde{\boldsymbol{\Psi}}$: coherence matrix
- $\tilde{\mathbf{w}}_\theta$: vector of phase exponential

Gaussian distribution



Consider a set $\{\tilde{\mathbf{x}}^i\}_{i=1}^n$ with $\tilde{\mathbf{x}}^i \in \mathbb{C}^p$ for all $i \in [1, n]$, independently and identically distributed.
 $\tilde{\mathbf{x}} \sim \mathcal{CN}(0, \Sigma)$

The log-likelihood is

$$\begin{aligned}\mathcal{L}(\tilde{\mathbf{x}}; \Sigma) &= -\log \left(\prod_{i=1}^n f(\tilde{\mathbf{x}}^i, \Sigma) \right) \\ &\propto n \log(|\Sigma|) + n \text{Tr}(\Sigma^{-1} \mathbf{S})\end{aligned}$$

$$\text{where } \mathbf{S} = \frac{1}{n} \sum_{i=1}^n \tilde{\mathbf{x}}^i \tilde{\mathbf{x}}^{iH}$$

$$n > p$$

Figure: Representation of time series of SAR data with a sliding window containing n pixels $\tilde{\mathbf{x}}^i$ [1]

Classic Phase Linking (PL)

Principle:

- Estimate $p - 1$ phase differences from p SAR images.
- Estimate average velocities and time series of displacements.

Assuming that $\tilde{\Psi}$ is known (plug-in: $\tilde{\Psi}_{mod} = |\mathbf{S}|$), the method is equivalent to optimizing the following problem [2] :

$$\begin{aligned} & \underset{\tilde{\mathbf{w}}_{\theta}}{\text{minimize}} && \tilde{\mathbf{w}}_{\theta}^H (\tilde{\Psi}^{-1} \circ \mathbf{S}) \tilde{\mathbf{w}}_{\theta} \\ & \text{subject to} && \theta_1 = 0 \end{aligned} \tag{2}$$

Content

- ① SAR interferometry
- ② Phase Linking (PL)
- ③ Sequential problematic
- ④ Covariance fitting interferometric PL (COFI-PL)
 - Offline approach
 - Online approach
- ⑤ PL based on maximum likelihood estimation (MLE-PL)
 - Offline approach
 - Online approach
- ⑥ Conclusion and perspectives

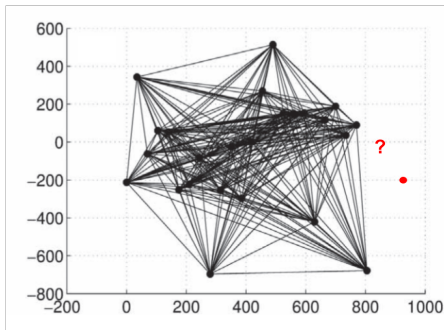
Sequential problematic

New data is coming in: the size of the data vector is increasing

$$\forall i = 1, \dots, n \quad \tilde{\mathbf{x}}^i = (\mathbf{x}^i)_{(p,1)} \rightarrow \tilde{\mathbf{x}}^i = \begin{pmatrix} \mathbf{x}^i \\ \mathbf{x}_{p+1}^i \end{pmatrix}_{(p+1,1)}$$

The Phase Linking MT-InSAR approaches
redone on all the data

- Computation time
- memory
- learning support



Problem : Development of a new, robust and sequential multi-temporal SAR interferometry approach for estimating SAR phase time series using statistical tools.

Content

- 1 SAR interferometry
- 2 Phase Linking (PL)
- 3 Sequential problematic
- 4 Covariance fitting interferometric PL (COFI-PL)
 - Offline approach
 - Online approach
- 5 PL based on maximum likelihood estimation (MLE-PL)
 - Offline approach
 - Online approach
- 6 Conclusion and perspectives

Content

- 1 SAR interferometry
- 2 Phase Linking (PL)
- 3 Sequential problematic
- 4 Covariance fitting interferometric PL (COFI-PL)
 - Offline approach
 - Online approach
- 5 PL based on maximum likelihood estimation (MLE-PL)
 - Offline approach
 - Online approach
- 6 Conclusion and perspectives

Problem reformulation

Classic PL optimization problem [2]

$$\begin{aligned} & \underset{\tilde{\mathbf{w}}_\theta}{\text{minimize}} && \tilde{\mathbf{w}}_\theta^H (\tilde{\boldsymbol{\Psi}}^{-1} \circ \mathbf{S}) \tilde{\mathbf{w}}_\theta \\ & \text{subject to} && \theta_1 = 0 \end{aligned}$$

Covariance fitting interferometric PL (COFI-PL) involves refining the structure of the covariance matrix estimator by minimizing a projection criterion.

The fitting problem can be reformulated as [3]

$$\begin{aligned} & \underset{\tilde{\mathbf{w}}_\theta}{\text{minimize}} && f(\tilde{\boldsymbol{\Sigma}}, \tilde{\boldsymbol{\Psi}} \odot \tilde{\mathbf{w}}_\theta \tilde{\mathbf{w}}_\theta^H) \\ & \text{subject to} && \theta_1 = 0 \\ & && \tilde{\mathbf{w}}_\theta \in \mathbb{T}_p \end{aligned} \tag{3}$$

with $\mathbb{T}_p = \{\mathbf{w} \in \mathbb{C}^p | |[w]_i| = 1, \forall i \in [1, p]\}$

Solution

- Majorization-Minimization (MM) algorithm
- Riemannian gradient descent algorithm

[2] Guarnieri, Andrea Monti, and Stefano Tebaldini. "On the exploitation of target statistics for SAR interferometry applications." IEEE Transactions on Geoscience and Remote Sensing 46.11 (2008): 3436-3443.

[3] Vu, Phan Viet Hoa, et al. "Covariance Fitting Interferometric Phase Linking: Modular Framework and Optimization Algorithms." arXiv preprint arXiv:2403.08646 (2024).

Matrix distances

- Kullback-Leibler divergence : $f_{\tilde{\Sigma}}^{KL}(\tilde{\mathbf{w}}_\theta) = \tilde{\mathbf{w}}_\theta^H (\tilde{\Psi}^{-1} \odot \tilde{\Sigma}) \mathbf{w}_\theta$
- Frobenius norm : $f_{\tilde{\Sigma}}^{LS}(\tilde{\mathbf{w}}_\theta) = -2\tilde{\mathbf{w}}_\theta^H (\tilde{\Psi} \odot \tilde{\Sigma}) \tilde{\mathbf{w}}_\theta$
- ...

Covariance estimation

- SCM : $\tilde{\Sigma} = \frac{1}{n} \sum_{i=1}^n \tilde{\mathbf{x}}^i \tilde{\mathbf{x}}^{iH}$
- Phase-Only : $\tilde{\Sigma} = \frac{1}{n} \sum_{i=1}^n \tilde{\mathbf{y}}^i \tilde{\mathbf{y}}^{iH}$ with $\tilde{\mathbf{y}} = \phi(\tilde{\mathbf{x}})$ with $\Phi : \tilde{x} = \gamma e^{i\theta} \rightarrow e^{i\theta}$
- Shrinkage to identity : $\tilde{\Sigma}(\beta) = \beta \hat{\Sigma} + (1 - \beta) \frac{\text{tr}(\hat{\Sigma})}{p} \mathbf{I}$ with $\beta \in [0, 1]$
- Covariance matrix tapering : $\tilde{\Sigma}(\beta) = \mathbf{W}(b) \odot \hat{\Sigma}$ with $[\mathbf{W}(b)]_{ij} = \begin{cases} 1 & \text{if } |i - j| \leq b \\ 0 & \text{otherwise} \end{cases}$

Content

1 SAR interferometry

2 PL

3 Sequential problematic

4 COFI-PL

- Offline approach
- **Online approach**

5 PL based on maximum likelihood estimation (MLE-PL)

- Offline approach
- Online approach

6 Conclusion and perspectives

Data model

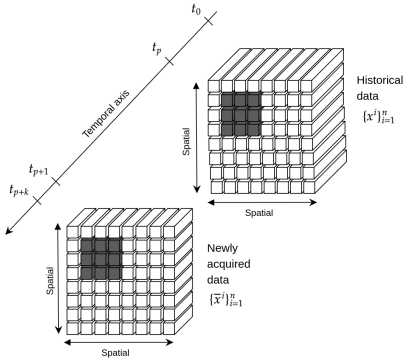


Figure: Representation of time series of SAR data with a sliding window containing n pixels $\tilde{\mathbf{x}}^i$.

We consider a set $\{\tilde{\mathbf{x}}^i\}_{i=1}^n$ where

$$\tilde{\mathbf{x}}^i = [\underbrace{\mathbf{x}_1^i, \dots, \mathbf{x}_p^i}_{\mathbf{x}^i}, \underbrace{\mathbf{x}_{p+1}^i, \dots, \mathbf{x}_{p+k}^i}_{\tilde{\mathbf{x}}^i}]^T \in \mathbb{C}^{p+k} \quad (4)$$

Each pixel of the local patch is assumed to be distributed as a zero mean Complex Circular Gaussian (CCG), i.e., $\tilde{\mathbf{x}} \sim \mathcal{CN}(0, \tilde{\Sigma})$.
 The hermitian structured covariance matrix, given in (1), can be rewritten as

$$\tilde{\Sigma} = \begin{pmatrix} \Sigma_{\text{past}} & \mathbf{v}^H \\ \mathbf{v} & \mathbf{z} \end{pmatrix}_{(p+k, p+k)}$$

The coherence matrix $\tilde{\Psi}$ can be represented as follow :

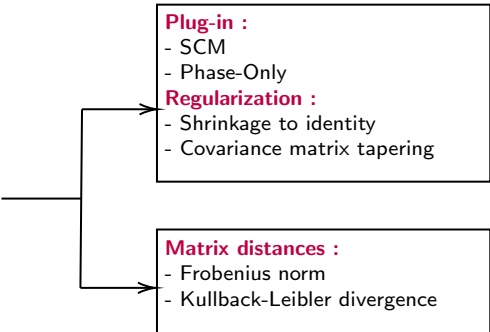
$$\tilde{\Psi} = \begin{pmatrix} \Psi_{\text{past}} & \mathbf{A}^T \\ \mathbf{A} & \mathbf{B} \end{pmatrix}_{(p+k, p+k)}$$

Problem formulation

The optimization problem is formalized as follow

$$\min_{\mathbf{w}_{\text{new}}} f(\tilde{\Sigma}, \tilde{\Psi} \circ \tilde{\mathbf{w}}_\theta \tilde{\mathbf{w}}_\theta^H)$$

subject to $\mathbf{w}_{\text{new}} \in \mathbb{T}_k$
 $\theta_1 = 0$



Solution

- MM algorithm
- Riemannian gradient descent algorithm

Optimization problem resolution - MM algorithm (1/2)

MM algorithm :

- ① majorizing the cost function by a $g(\cdot | \mathbf{w}_{\text{new}}^{(t)})$: $f(\mathbf{w}_{\text{new}}) \leq g(\mathbf{w}_{\text{new}} | \mathbf{w}_{\text{new}}^{(t)})$, $\forall \mathbf{w}_{\text{new}} \in \mathbb{T}_k$
- ② minimizing the obtained function $g(\mathbf{w}_{\text{new}} | \mathbf{w}_{\text{new}}^{(t)})$

Step 1:

Lemma

The concave quadratic form $f : \mathbf{w} \longrightarrow -\mathbf{w}^H \mathbf{H} \mathbf{w}$ is majorized by : $-Re(\mathbf{w}^H \mathbf{H} \mathbf{w}^{(t)})$ with equality at point $\mathbf{w}^{(t)}$ [3]

So $f_{\tilde{\Sigma}}^{LS}(\tilde{\Sigma}, \tilde{\Psi} \circ \mathbf{w}_\theta \mathbf{w}_\theta^H)$ is majorized by the following expression

$$g(\mathbf{w}_{\text{new}} | \mathbf{w}_{\text{new}}^{(t)}) = -Re(\mathbf{w}_{\text{new}}^H (4(\mathbf{A} \circ \mathbf{V}) \mathbf{w}_{\text{past}} + (\mathbf{B} \circ \mathbf{Z}) \mathbf{w}_{\text{new}}^{(t)})) \quad (5)$$

Optimization problem resolution - MM algorithm (2/2)

Step 2:

Lemma

The solution of the minimization problem

$$\min_{\mathbf{w} \in \mathbb{T}_k} -\text{Re}(\mathbf{w}^H \bar{\mathbf{w}}^{(t)})$$

is obtained as $\mathbf{w}^* = \Phi_{\mathbb{T}}(\bar{\mathbf{w}}^{(t)})$ with $\Phi : x = r e^{i\theta} \rightarrow e^{i\theta}$ [3]

The problem is equivalent to the following one :

$$\begin{aligned} \min_{\mathbf{w}_{\text{new}} \in \mathbb{T}_k} \quad & -\text{Re} \left(4 \mathbf{w}_{\text{new}}^H \left((\mathbf{A} \circ \mathbf{V}) \mathbf{w}_{\text{past}} + (\mathbf{B} \circ \mathbf{Z}) \mathbf{w}_{\text{new}}^{(t)} \right) \right) \\ & = -\text{Re}(\mathbf{w}_{\text{new}}^H \bar{\mathbf{w}}^{(t)}) \end{aligned} \tag{6}$$

and the solution is obtained as

$$\mathbf{w}_{\text{new}}^{(t)} = \Phi_{\mathbb{T}}(\bar{\mathbf{w}}^{(t)})$$

with $\Phi_{\mathbb{T}} : x = r e^{i\theta} \rightarrow e^{i\theta}$

Optimization problem resolution - Riemannian GD (1/2)

Manifold : torus of phase-only complex vector (\mathbb{T}_k)

$$\mathbb{T}_k = \{\mathbf{w} \in \mathbb{C}^k \mid |[w]_i| = 1, \forall i \in [1, k]\}$$

Tangent space : at point \mathbf{w} , $T_{\mathbf{w}}\mathbb{T}_k$

$$T_{\mathbf{w}}\mathbb{T}_k = \{\xi \in \mathbb{C}^k \mid \text{Re}\{\xi \odot \mathbf{w}\} = 0\}$$

By endowing each tangent space with the Euclidean metric, \mathbb{T}_k becomes a Riemannian submanifold

$$\begin{aligned} <.,.\rangle_{\mathbf{w}} : T_{\mathbf{w}}\mathbb{T}_k \times T_{\mathbf{w}}\mathbb{T}_k &\rightarrow \mathbb{R} \\ \xi, \eta &\rightarrow \text{Re}\{\xi^H \eta\} \end{aligned} \tag{7}$$

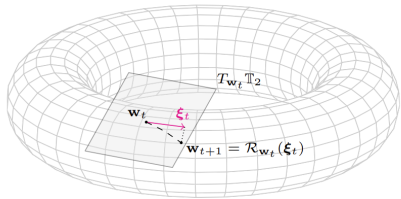


Figure: Illustration of Riemannian optimization on \mathbb{T}_2 (represented as a torus embedded in \mathbb{R}^3): the iterate \mathbf{w}_{t+1} is obtained from the retraction $R_{\mathbf{w}_t}$ applied to the direction descent $\xi_t \in T_{\mathbf{w}_t}\mathbb{T}_2$ (i.e., a vector of the tangent space of \mathbb{T}_2 at point \mathbf{w}_t). [3]

Optimization problem resolution - Riemannian GD (2/2)

Step 1 :

Euclidean gradient :

$$\nabla f(\mathbf{w}_{\text{new}}^{(t)}) = -4 \left((\mathbf{A} \circ \mathbf{V}) \mathbf{w}_{\text{past}} + (\mathbf{B}^T \circ \mathbf{Z}^H) \mathbf{w}_{\text{new}}^{(t)} \right) \quad (8)$$

The Riemannian gradient the function $f : \mathbb{T}_k \rightarrow \mathbb{R}$ at point $\mathbf{w}_{\text{new}}^{(t)}$ is the unique vector defined as

$$\langle \text{grad } f(\mathbf{w}_{\text{new}}^{(t)}), \xi \rangle_{\mathbf{w}_{\text{new}}^{(t)}} = D f(\mathbf{w}_{\text{new}}^{(t)})[\xi] \quad (9)$$

Step 2 :

Defining the retraction operator $R_{\mathbf{w}_{\text{new}}^{(t)}} : T_{\mathbf{w}_{\text{new}}^{(t)}} \mathbb{T}_k \rightarrow \mathbb{T}_k$, that maps tangent vectors back to the manifold. The euclidean projection on \mathbb{T}_k is a practical candidate.

$$R_{\mathbf{w}_{\text{new}}^{(t)}}(\xi^{(t)}) = \Phi_{\mathbb{T}}(\mathbf{w}_{\text{new}}^{(t)} + \xi^{(t)}) \quad (10)$$

with $\Phi : x = \gamma e^{i\theta} \rightarrow e^{i\theta}$

Update $\mathbf{w}_{\text{new}}^{(t+1)} = R_{\mathbf{w}_{\text{new}}^{(t)}}(\xi^{(t)})$

Simulation - Computation Time

Simulation parameters

- $\tilde{\Psi}$: Toeplitz matrix with coherence coefficient $\rho = 0.7$
- $p + 1 = 20$ SAR phases: random values in $[-\pi, \pi]$
- Covariance matrix : $\tilde{\Sigma} = \text{diag}(\tilde{\mathbf{w}}_\theta)\tilde{\Psi}\text{diag}(\tilde{\mathbf{w}}_\theta)^H$
- n i.i.d samples simulated following the $\mathcal{CN}(0, \tilde{\Sigma})$

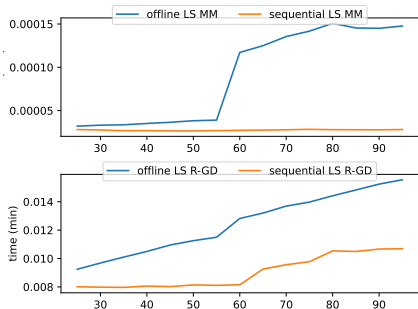


Figure: Computation time variation versus p , $n = 2 \times (p + k)$ for MM and R-GD

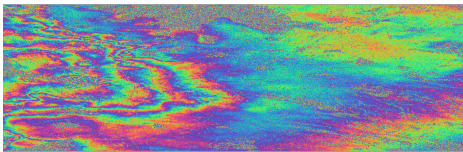
Real data - Mexico city



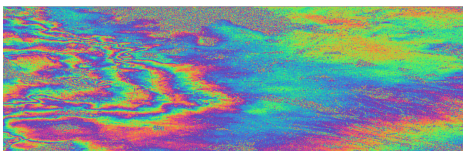
- Mexico City, with a population exceeding 20 million, ranks among the most dynamic cities in the world.
 - The rapid urbanization of Mexico City has resulted in a significant increase in demand for water.
 - The primary water supply for Mexico City comes from aquifers, leading to subsidence and deformation across the city.

Figure: Mexico City

Real data - Results



(a) COFI-PL



(b) S-COFI-PL

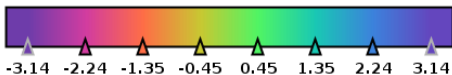


Figure: Close-up view of interferograms (14 August 2019 - 10 April 2020) estimated by (a) COFI-PL, and (b) S-COFI-PL in case $p + 1 = 20$ and $n = 64$

Content

1 SAR interferometry

2 PL

3 Sequential problematic

4 COFI-PL

- Offline approach
- Online approach

5 PL based on maximum likelihood estimation (MLE-PL)

- Offline approach
- Online approach

6 Conclusion and perspectives

Content

1 SAR interferometry

2 PL

3 Sequential problematic

4 COFI-PL

- Offline approach
- Online approach

5 PL based on maximum likelihood estimation (MLE-PL)

- Offline approach
- Online approach

6 Conclusion and perspectives

PL based on maximum likelihood estimation

Classic PL optimization problem

$$\begin{aligned} & \underset{\tilde{\mathbf{w}}_\theta}{\text{minimize}} \quad \tilde{\mathbf{w}}_\theta^H (\tilde{\boldsymbol{\Psi}}^{-1} \circ \mathbf{S}) \tilde{\mathbf{w}}_\theta \\ & \text{subject to} \quad \theta_1 = 0 \end{aligned}$$

PROBLEM !!! In reality, $\tilde{\boldsymbol{\Psi}}$ is unknown.
→ [1] proposed to estimate $\tilde{\boldsymbol{\Psi}}$ jointly with $\tilde{\mathbf{w}}_\theta$.

→ The optimization problem [1]:

$$\begin{aligned} & \underset{\tilde{\boldsymbol{\Psi}}, \tilde{\mathbf{w}}_\theta}{\text{minimize}} \quad \mathcal{L}_G(\tilde{\boldsymbol{\Sigma}}(\tilde{\boldsymbol{\Psi}}, \tilde{\mathbf{w}}_\theta)) = n \log(|\tilde{\boldsymbol{\Sigma}}|) + \sum_{i=1}^n \tilde{\mathbf{x}}^{iH} \tilde{\boldsymbol{\Sigma}}^{-1} \tilde{\mathbf{x}}^i \\ & \text{subject to} \quad \theta_1 = 0, \tilde{\mathbf{w}}_\theta \in \mathbb{T}_p, \tilde{\boldsymbol{\Psi}} \text{ real symmetric} \end{aligned}$$

with $\mathbb{T}_p = \{\mathbf{w} \in \mathbb{C}^p | |[\tilde{\mathbf{w}}]_i| = 1, \forall i \in [1, p]\}$

2 unknowns to estimate → **Block Coordinate Descent Algorithm (BCD)**

- **Update $\tilde{\boldsymbol{\Psi}}$** : Minimize \mathcal{L}_G with fixed $\tilde{\mathbf{w}}_\theta$
- **Update $\tilde{\mathbf{w}}_\theta$** : Minimize \mathcal{L}_G with fixed $\tilde{\boldsymbol{\Psi}}$ → Phase Linking

The minimization problem above is solved using the majorization-minimization (MM) algorithm.

+ Extension to Non-Gaussian model [4]

[1] Vu, Phan Viet Hoa, et al. "A new phase linking algorithm for multi-temporal INSAR based on the maximum likelihood estimator." IGARSS 2022-2022 IEEE International Geoscience and Remote Sensing Symposium. IEEE, 2022.

[4] P. Vu, A. Breloy, F. Brigui, Y. Yan, and G. Ginolhac. Robust phase linking in insar.IEEE Transactions on Geoscience and Remote Sensing, 2023

Content

- ① SAR interferometry
- ② PL
- ③ Sequential problematic
- ④ COFI-PL
 - Offline approach
 - Online approach
- ⑤ PL based on maximum likelihood estimation (MLE-PL)
 - Offline approach
 - **Online approach**
- ⑥ Conclusion and perspectives

Data model

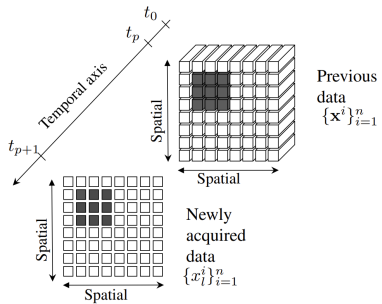


Figure: Representation of time series of SAR data with a sliding window containing n pixels $\tilde{\mathbf{x}}^i$ [5]

We consider a set $\{\tilde{\mathbf{x}}^i\}_{i=1}^n$ where

$$\tilde{\mathbf{x}}^i = \underbrace{[x_1^i, \dots, x_p^i]}_{\mathbf{x}^i}, x_p^i \in \mathbb{C}^{l=p+1} \quad (11)$$

Each pixel of the local patch is assumed to be distributed as a zero mean CCG, i.e., $\tilde{\mathbf{x}} \sim \mathcal{CN}(0, \tilde{\Sigma})$.

The hermitian structured covariance matrix, given in (1), can be rewritten as

$$\tilde{\Sigma} = \begin{pmatrix} \sum_{past} & w_{\theta_I}^* diag(w_{\theta_I}) \gamma^T \\ \gamma diag(w_{\theta_I})^H w_{\theta_I} & \gamma I \end{pmatrix} \quad (12)$$

MLE problem

The associated negative log-likelihood for the entire dataset, can be expressed as

$$\mathcal{L}_G(\tilde{\mathbf{x}}^i; \boldsymbol{\gamma}, \boldsymbol{\gamma}_I, \mathbf{w}_{\theta_I}) = - \sum_{i=1}^n \mathcal{L}_G^i(\mathbf{x}_I^i | \mathbf{x}^i; \boldsymbol{\gamma}, \boldsymbol{\gamma}_I, \mathbf{w}_{\theta_I}) + \mathcal{L}_G^i(\mathbf{x}^i) \quad (13)$$

According to [6], $\mathbf{x}_I^i | \mathbf{x}^i \sim \mathcal{CN}(\mu_x^i, \sigma_x^2)$ where

$$\begin{aligned}\mu_x^i &= \mathbf{w}_{\theta_I} \boldsymbol{\gamma} \text{diag}(\hat{\mathbf{w}}_\theta)^H \hat{\boldsymbol{\Sigma}}_{past}^{-1} \mathbf{x}^i, \\ \sigma_x^2 &= \boldsymbol{\gamma}_I - \boldsymbol{\gamma} \text{diag}(\hat{\mathbf{w}}_\theta)^H \hat{\boldsymbol{\Sigma}}_{past}^{-1} \text{diag}(\hat{\mathbf{w}}_\theta^H) \boldsymbol{\gamma}^T,\end{aligned}$$

and the negative log-likelihood in (13), can be formulated as

$$\mathcal{L}_G(\tilde{\mathbf{x}}^i; \boldsymbol{\gamma}, \boldsymbol{\gamma}_I, \mathbf{w}_{\theta_I}) \propto n \log(v) + \sum_{i=1}^n \frac{y^{i*} y^i}{v}. \quad (14)$$

$$\begin{aligned}\text{where } y^i &= \mathbf{x}_I^i - \mathbf{w}_{\theta_I} \boldsymbol{\gamma} \text{diag}(\hat{\mathbf{w}}_\theta)^H \hat{\boldsymbol{\Sigma}}_{past}^{-1} \mathbf{x}^i \\ \text{and } v &= \boldsymbol{\gamma}_I - \boldsymbol{\gamma} \text{diag}(\hat{\mathbf{w}}_\theta)^H \hat{\boldsymbol{\Sigma}}_{past}^{-1} \text{diag}(\hat{\mathbf{w}}_\theta) \boldsymbol{\gamma}^T\end{aligned}$$

MLE problem

The associated optimization problem has the following form

$$\begin{aligned} \min_{\gamma, \gamma_I, w_{\theta_I}} \quad & \mathcal{L}_{\mathcal{G}}(\tilde{\mathbf{x}}^i; \gamma, \gamma_I, w_{\theta_I}) \\ \text{subject to} \quad & \gamma, \gamma_I \text{ real}, |w_{\theta_I}| = 1, \theta_1 = 0 \end{aligned} \tag{15}$$

and will be addressed using a **Block Coordinate Descent (BCD)** algorithm.

- **Update γ** : Minimize $\mathcal{L}_{\mathcal{G}}$ with fixed $w_{\theta_{p+1}}$ and γ_{p+1}

$$\gamma = \left(\sum_{i=1}^n w_{\theta_I}^* x_I^i \mathbf{L}^i - w_{\theta_I} x_I^{i*} \mathbf{L}^{i*} \right) \cdot \left(\sum_{i=1}^n \mathbf{M}^i + \mathbf{M}^{i*} \right)^{-1}$$

where $\mathbf{L}^i = \mathbf{x}^{iH} \hat{\Sigma}_{past}^{-1} \text{diag}(\hat{\mathbf{w}}_{\theta})$ and $\mathbf{M}^i = \mathbf{L}^{iH} \mathbf{L}^i$

- **Update γ_I** : Minimize $\mathcal{L}_{\mathcal{G}}$ with fixed $w_{\theta_{p+1}}$ and γ

$$\gamma_I = \frac{1}{n} \sum_{i=1}^n (x_I^i - w_{\theta_I} \gamma \mathbf{L}^{iH})^* (x_I^i - w_{\theta_I} \gamma \mathbf{L}^{iH}) + \gamma \mathbf{N} \gamma^T$$

where $\mathbf{N} = \text{diag}(\hat{\mathbf{w}}_{\theta})^H \hat{\Sigma}_{past}^{-1} \text{diag}(\hat{\mathbf{w}}_{\theta})$

- **Update w_{θ_I}** : Minimize $\mathcal{L}_{\mathcal{G}}$ with fixed γ_{p+1} and γ

$$w_{\theta_I} = \frac{\left((\sum_{i=1}^n x_I^i \mathbf{L}^i \gamma^T) \cdot (\sum_{i=1}^n \gamma \mathbf{M}^i \gamma^T)^{-1} \right)}{\| \left((\sum_{i=1}^n x_I^i \mathbf{L}^i \gamma^T) \cdot (\sum_{i=1}^n \gamma \mathbf{M}^i \gamma^T)^{-1} \right) \|}$$

Simulation - Computation Time

Simulation parameters

- $\tilde{\Sigma}$: Toeplitz matrix with coherence coefficient $\rho = 0.7$
- $p + 1 = 20$ SAR phases: random values in $[-\pi, \pi]$
- Covariance matrix : $\tilde{C} = \text{diag}(\tilde{w}_\theta) \tilde{\Sigma} \text{diag}(\tilde{w}_\theta)^H$
- n i.i.d samples simulated following the $\mathcal{CN}(0, \tilde{C})$

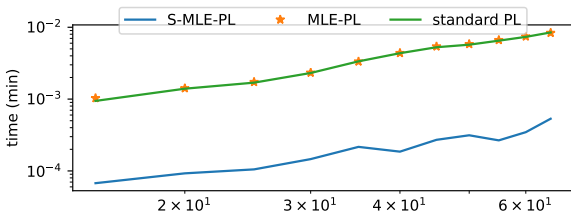
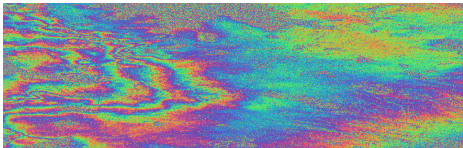
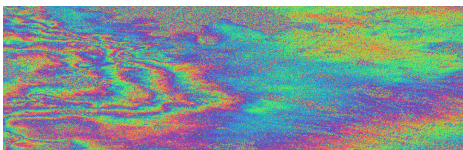


Figure: Computation time variation versus p , $n = 2 \times (p + 1)$

Real data - Results



(a) MLE-PL



(b) S-MLE-PL

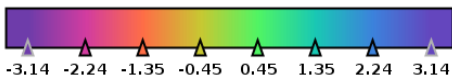


Figure: Close-up view of interferograms (14 August 2019 - 10 April 2020) estimated by (a) MLE-PL, and (b) S-MLE-PL in case $p + 1 = 20$ and $n = 64$

1 SAR interferometry

2 PL

3 Sequential problematic

4 COFI-PL

- Offline approach
- Online approach

5 MLE-PL

- Offline approach
- Online approach

6 Conclusion and perspectives

Conclusion and perspectives

Conclusion

Two sequential approaches that efficiently incorporate new SAR images in interferometric phase estimation within a PL framework :

- same level of performance as offline methods
- reduced computational costs compared to traditional offline approaches

Perspectives

- Generalization of S-MLE-PL to a bloc of new SAR images
- proceed to step 2 : estimate the displacement time series and compare the results with GPS data

References

- [1] P. Vu, F. Brigui, A. Breloy, Y. Yan, and G. Ginolhac. A new phase linking algorithm for multi-temporal insar based on the maximum likelihood estimator. In *IGARSS 2022-2022 IEEE International Geoscience and Remote Sensing Symposium*, pages 76–79. IEEE, 2022.
- [2] A. Guarnieri and S. Tebaldini. On the exploitation of target statistics for sar interferometry applications. *IEEE Transactions on Geoscience and Remote Sensing*, 46(11):3436–3443, 2008.
- [3] P. Vu, A. Breloy, F. Brigui, Y. Yan, and G. Ginolhac. Covariance fitting interferometric phase linking: Modular framework and optimization algorithms. *arXiv preprint arXiv:2403.08646*, 2024.
- [4] P. Vu, A. Breloy, F. Brigui, Y. Yan, and G. Ginolhac. Robust phase linking in insar. *IEEE Transactions on Geoscience and Remote Sensing*, 2023.
- [5] D. El hajjar, Y. Yan, G. Ginolhac, and M.N. El korso. Sequential phase linking: progressive integration of sar images for operational phase estimation. In *IGARSS 2024 IEEE International Geoscience and Remote Sensing Symposium*. IEEE, 2024 (accepted).
- [6] T. W. Anderson. An introduction to multivariate statistical analysis. Technical report, 1962.

COFI-PL problem resolution : MM algorithm

Algorithm MM for Kullback-Leibler divergence

- 1: **Input:** $\tilde{\Sigma} \in \mathbb{C}^p$, $w^{(1)} \in \mathbb{T}_p$
 - 2: Compute : $\mathbf{M} = \text{mod}(\tilde{\Sigma})^{-1} \odot \tilde{\Sigma}$ and $\lambda_{\max}^{\mathbf{M}}$
 - 3: **repeat**
 - 4: Compute $\bar{w}^{(t)} = (\lambda_{\max}^{\mathbf{M}} \mathbf{I} - \mathbf{M}) w^{(t)}$
 - 5: Update of $w^{(t)} = \phi_{\mathbb{T}}\{\bar{w}^{(t)}\}$
 - 6: $t = t + 1$
 - 7: **until** convergence
 - 8: **Output:** $\hat{w}_{\theta} = \mathbf{w}_{end} \in \mathbb{T}_p$
-

Algorithm MM for Frobenius Norm

- 1: **Input:** $\tilde{\Sigma} \in \mathbb{C}^p$, $w^{(1)} \in \mathbb{T}_p$
 - 2: Compute : $\mathbf{M} = \text{mod}(\tilde{\Sigma}) \odot \tilde{\Sigma}$
 - 3: **repeat**
 - 4: Compute $\bar{w}^{(t)} = \mathbf{M} w^{(t)}$
 - 5: Update of $w^{(t)} = \phi_{\mathbb{T}}\{\bar{w}^{(t)}\}$
 - 6: $t = t + 1$
 - 7: **until** convergence
 - 8: **Output:** $\hat{w}_{\theta} = \mathbf{w}_{end} \in \mathbb{T}_p$
-

COFI-PL problem resolution : Riemannian optimization on \mathbb{T}_p

$$\begin{aligned} & \underset{\mathbf{w}_\theta}{\text{minimize}} && f(\tilde{\Sigma}, \tilde{\Psi} \odot \tilde{\mathbf{w}}_\theta \tilde{\mathbf{w}}_\theta^H) \\ & \text{subject to} && \theta_1 = 0 \\ & && \tilde{\mathbf{w}}_\theta \in \mathbb{T}_p \end{aligned}$$

Algorithm Riemannian gradient descent algorithm

Input: Objective function f of problem (40), starting point \mathbf{w}_0

repeat

 Compute euclidean gradient

 Compute riemannian gradient

 Set direction $\xi^{(t)} = -\alpha \eta^{(t)}$

 Update $\mathbf{w}^{(t)} = \mathcal{R}_{\mathbf{w}^{(t)}}(\xi^{(t)})$

until convergence

Output: $\hat{\mathbf{w}}_\theta = \mathbf{w}_{end} \in \mathbb{T}_p$

Appendix - S-COFI-PL simulations

Simulation parameters

- $\tilde{\Sigma}$: Toeplitz matrix with coherence coefficient $\rho \in [0.5, 0.7, 0.9]$
- $p + 1 = 20$ SAR phases: random values in $[-\pi, \pi]$
- Covariance matrix : $\tilde{C} = \text{diag}(\tilde{w}_\theta)\tilde{\Sigma}\text{diag}(\tilde{w}_\theta)^H$
- n i.i.d samples simulated following the $\mathcal{CN}(0, \tilde{C})$

Simulation results

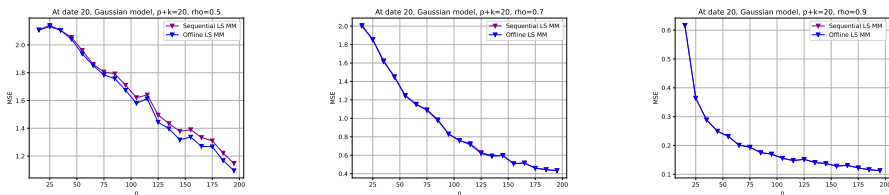
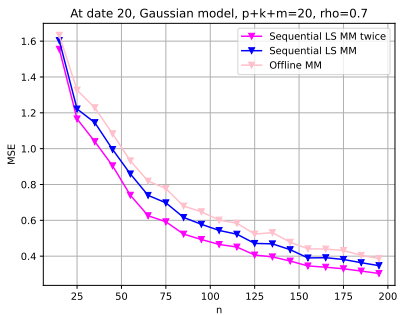
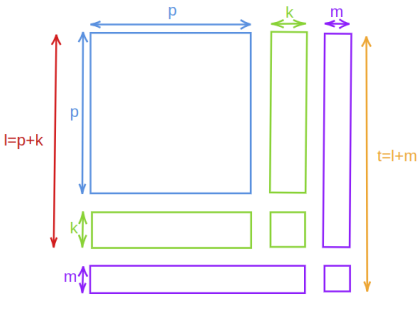


Figure: MSE of InSAR phases estimates using COFI-PL and sequential method with Gaussian distributed input data. $p + 1 = 20$, $\rho \in [0.5, 0.7, 0.9]$, 1000 Monte Carlo trials

Appendix - Sequential integration of several new images



Appendix - S-MLE-PL simulations

Simulation parameters

- $\tilde{\Sigma}$: Toeplitz matrix with coherence coefficient $\rho \in [0.5, 0.7, 0.9]$
- $p + 1 = 20$ SAR phases: random values in $[-\pi, \pi]$
- Covariance matrix : $\tilde{C} = \text{diag}(\tilde{w}_\theta) \tilde{\Sigma} \text{diag}(\tilde{w}_\theta)^H$
- n i.i.d samples simulated following the $\mathcal{CN}(0, \tilde{C})$

Approaches to be compared

- $2p - InSAR$: phase estimated from n - pixel averaged interferograms formed with respect to the first image
- Classic PL
- MLE-PL
- S-MLE-PL (our approach)

Appendix - S-MLE-PL simulations results

Gaussian distributed input data

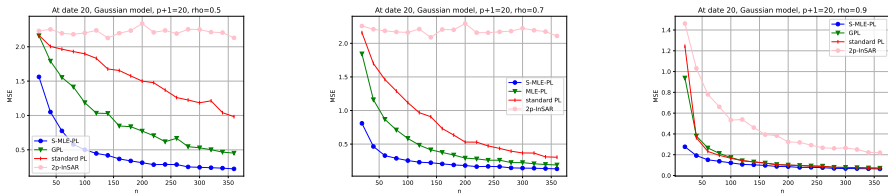


Figure: MSE of InSAR phases estimates using 2p-InSAR, classic PL and MLE-PL and sequential method with Gaussian distributed input data. $p + 1 = 20$, $\rho \in [0.5, 0.7, 0.9]$, 1000 Monte Carlo trials

Appendix - Sequential integration of several new images

